Regulation of Protective Th17 Cells by P. UF1 Bacterium Against Intestinal Pathogenic Inflammation

Natacha Colliou, Yong Ge, Bikash Sahay, Minghao Gong, Mojgan Zadeh, Jennifer L. Owen, Josef Neu, William G Farmerie, Francis Alonzo III, Ken Liu, Dean P Jones, Shuzhao Li & Mansour Mohamadzadeh

Supplemental data includes:

Supplemental Methods

Supplemental References

Supplemental Tables S1and S2

Supplemental Figures 1 to 13

Supplemental Experimental Procedures

Preterm infants' microbiota analyses and fecal microbiota transfer into GF mice. Microbiota analyses were performed on the Illumina Miseq (Illumina, Inc., San Diego, CA), as outlined previously (1, 2) using primers, as previously described (3). Sequence analyses were performed using QIIME v.1.9.0 (4). Briefly, after checking quality of sequenced reads, 8 nucleotides (nt) barcodes were extracted from both forward and reverse reads to generate a barcode library. Forward and reverse reads were then joined. Sequence libraries were filtered, as previously described (4), and split based on their corresponding barcodes. We used an open reference operational taxonomic unit (OTU) picking strategy to select OTU (with 97% identity threshold) (5). Taxonomy was assigned based on the Greengenes reference database (6). After single alpha rarefaction based on rarefaction curve, alpha diversity (e.g., Chao diversity, Shannon diversity, Evenness index) was measured. Subsequently, a taxonomic table for each taxonomic level was generated based on the OTU table. The phylum level taxonomic table was the basis for the phylum pie chart depiction. Differentially significant features at each level were identified using linear discriminant analysis (LDA) along with effect size measurements (LEfSe) (7). The significant taxons were filtered by LDA Effect Size (LEfSe) analyses with default criteria ($P < 0.05$ by Kruskal-Wallis test; LDA score > 2). The LEfSe data were further used for cladogram depiction using Graphlan (8). For the studies involving transfaunation of GF mice, pooled fecal samples collected from HBMF or FF preterm infants were dissolved in reduced sterile PBS, and animals subsequently gavaged with 100 μL of the fecal slurry on day 0. A group of GF mice was gavaged every third day with P. UF1 (10^9 CFU/mouse) on days 1, 4, 7, and 10.

Bacterial strains and bacterial products. *Escherichia coli* NEB 5-alpha (New England BioLabs, MA) was used for plasmid construction and grown in Luria-Bertani (LB) medium at 37°C. The P. UF1 and its genetically modified strains were grown at 30°C in MRS medium (Difco Laboratories, Detroit, MI) supplemented with 1% (w/v) sodium lactate (Thermo Fisher Scientific, Rockford, USA) in an anaerobic chamber (Model AS-580, Anaerobe Systems, Morgan, Hill, CA). The transformations of the P. UF1 were performed, as described previously (9). The Δ*actA Listeria monocytogenes* (*L. m*) strains were grown in Brain Heart Infusion (BHI) (Difco Laboratories, Detroit, MI) medium at 37°C. Antibiotics were added at the following final concentrations: 5 µg/mL chloramphenicol and 1 mg/mL hygromycin B for P. UF1 strains; 200 µg/mL streptomycin and 50 µg/mL kanamycin for *L. m*. Surface layer (S-layer) proteins were extracted from P. UF1 cultures by resuspension in guanidine hydrochloride (4 M) at 37°C for 30 min (10) . The supernatants containing S-layer were dialyzed using a 10 kDa cutoff Slide-A-Lyer® Dialysis Cassette (Thermo Fisher Scientific, Rockford, USA). The brushed off bacteria obtained during this process was assigned as S-layer^{-} P. UF1.

Peptide identification. The S-layer proteins of P. UF1 were separated by SDS-PAGE and analyzed by mass-spectroscopy (MS). Dihydrolipoamide acetyltransferase (DlaT) was one of the major S-layer proteins from which three 15-mer amino acid peptides, including DlaT 208-222 (VGSSVPAAPAAAPAA), DlaT 245-259 (VAPPAPVAPSAPVAA), and DlaT 109-123 (AAAPVAPPAPPAPAA), were selected and synthesized (Thermo Fisher, Ulm, Germany). These peptides demonstrated high affinity to MHCII using a web-based *in-silico* software (http://tools.immuneepitope.org/mhcii/).

Generation of P. UF1 strains. The insertional inactivation of the *dlaT* gene in P. UF1 was performed by a single crossover strategy (11). Briefly, a 516-bp internal fragment of *dlaT* was amplified from the P. UF1 genome using primers DlaT-F/DlaT-R. The chloramphenicol resistance gene (*cmR,* 1,512 bp) (9) was synthesized by GenScript Corporation (Piscataway, NJ). The resulting two fragments were cloned into a pUC18 plasmid, yielding suicide plasmid, pUCC-*dlaT*. Following transformation into P. UF1, the chloramphenicol resistant colonies were selected, and the Δ*dlaT* P. UF1 was confirmed by sequencing the *dlaT* locus amplified with primers P1/P2. The stability of the isogenic strains was ascertained under antibiotic-free conditions. For gene complementation, a novel shuttle vector (pYMZ) between *E. coli* and P. UF1 was first constructed. Briefly, a hygromycin B resistance gene (*hygB*, 1128 bp) resistance gene (12) and a pLME108 replicon (*rep*, 2,063 bp) (9) were synthesized and cloned into a pUC18 plasmid, resulting in the pYMZ plasmid. A fragment (2,145 bp) containing the intact *dlaT* gene and its native promoter (P_{dlaT}) was amplified from the P. UF1 chromosome using CdlaT-F/CdlaT-R primers, digested with XbaI/BamHI, and cloned into the pYMZ plasmid to generate pYMZ-*dlaT*. To complement the three DlaT peptides (3pep), a fragment (507 bp) encoding the 3pep was amplified with 3Pep-lap-F/3Pep-R primers, and the *dlaT* promoter region (361 bp) was amplified with CdlaT-F/3Pep-lap-R primers. The P_{dlaT}-3pep fragment was generated by overlap PCR, digested with XbaI/KpnI, and cloned into the pYMZ plasmid yielding pYMZ-3pep, which overexpressed the 3pep under control of the native *dlaT* promoter. The *dlaT*Δ3pep fragment was generated by several overlap extension PCRs. CdlaT-F/Pep1-lap-R and Pep1-lap-F/CdlaT-R primers were used to amplify the *dlaT*Δpep1 fragment by overlap extension PCR. PCR amplifications utilizing the CdlaT-F/Pep2-lap-R and Pep2-lap-F/CdlaT-R primers and the template, *dlaT*Δpep1, resulted in the fragment, *dlaT*Δpep1Δpep2. Finally,

*dlaT*Δ3pep was generated by overlap PCR using CdlaT-F/Pep3-lap-R and Pep3-lap-F/CdlaT-R primers, and the *dlaT*Δpep1Δpep2 template. The purified *dlaT*Δ3pep fragment was digested with XbaI/BamHI and cloned into the pYMZ plasmid, generating pYMZ-*dlaT*Δ3pep. Plasmids, including pYMZ-*dlaT*, pYMZ-3pep, and pYMZ-*dlaT*Δ3pep, were electroporated into the Δ*dlaT* P. UF1 strain, resulting in transgenic strains, P. UF1-1, P. UF1-2, and P. UF1-3, respectively. The complemented strains were confirmed by restriction digestion and DNA sequencing of the plasmids isolated from corresponding recombinant P. UF1 strains. The oligonucleotides used in this study are listed in Table S2.

RNA isolation and quantitative reverse-transcription PCR (qRT-PCR). For analyses of *Socs1* expression, BMDCs isolated from *Signr1*$^{+/+}$ and *Signr1*$^{-/-}$ mice were pretreated with MEK inhibitor PD0325901 (5 μM) (Sigma Aldrich, St. Louis, MO) for 30 minutes before co-incubation with P. UF1 for 1, 3 or 6 hr. Total RNA was extracted from P. UF1 bacterial culture (1 mL, OD_{600} = 0.8) or ~ 0.5 cm length of intestinal tissues or BMDCs using Trizol reagents (Invitrogen Life Technologies) and purified by Aurum mini columns (Bio-Rad, Hercules, CA). DNA contaminants were completely removed by on-column digestion with DNase I (Bio-Rad, Hercules, CA). To quantify expression of *IL-1b*, *IL-6* and *IL-12/23p40*, colonic DCs were magnetically sorted and RNA was purified using RNeasy Plus Micro Kit (Qiagen, Germantown, MD). The cDNA was synthesized using iScript cDNA Synthesis Kit (Bio-Rad, Hercules, CA), and qPCR was carried out using SsoAdvanced Universal SYBR Green Supermix (Bio-Rad, Hercules, CA) on a CFX96 real-time PCR system (Bio-Rad, Hercules, CA). For each sample, qPCR was assayed in technical triplicate, and for each reaction, the calculated C_T value was normalized to the C_T of *GroL2* (for bacteria) or *Gapdh* (for murine tissues or cells) amplified

from the corresponding samples. Results are shown as a fold reduction relative to expression levels in PBS, Δ*actA L. m* infected tissues, or P. UF1 strain, as indicated.

Expression and purification of DlaT protein. For expression of DlaT protein by P. UF1, the DlaT-coding sequence was PCR amplified from P. UF1 chromosome using DlaT-F6/DlaT-R6 primers. The *Propionibacterium* strong promoter P4 (9), a synthetic ribosome-binding site (sRBS, sequence 5'TATTACTCCAGAAATACTACAGAAGGAGGAATTCC-3'), and DNA encoding six histidines (His_6) and the factor Xa cleavage site (sequence 5'-ATGGGCTCGTCGCACCACCACCACCACCACTCGTCGGGCATCGAGGGCCGC-3') were synthesized by GenScript Corporation (Piscataway, NJ) and cloned into plasmid pYMZ upstream from the *dlaT* gene. The resultant expression plasmid pYMZ-P4-*dlaT* was electroporated into P. UF1, and the expresser strain was identified by sequencing the plasmid isolated from the P. UF1 transformant. The recombinant bacteria were grown anaerobically in MRS-lactate medium without antibiotics at 30°C to an OD_{600} of ~3.0. The bacteria were pelleted by centrifugation, resuspended in protein binding buffer (20 mM NaPi, 500 mM NaCl, 20 mM imidazole, pH 7.4), and disrupted by sonication. The cell lysates were clarified by centrifugation and the supernatants were purified by immobilized metal affinity chromatography (IMAC) using AKTA Start purification system with a HisTrap HP column (GE Healthcare). Fractions containing His_6-DlaT proteins were pooled and exchanged into a buffer containing 20 mM Tris-HCl and 100 mM NaCl (pH 8.0) using an Amicon Ultral-15 centrifugal filter (Millipore, Temecula, CA). The protein preparations were further purified by anion exchange chromatography using a HiTrap Q Fast Flow column (GE Healthcare). The elution fractions were pooled, concentrated, and loaded onto a HiLoad Superdex 200 16/60 column (GE

Healthcare) preequilibrated with 50 mM NaPi, 150 mM NaCl, pH 7.4. Elution fractions containing His_6-DlaT proteins were concentrated to approximately 3-5 mg/mL for storage at -80°C. The purified proteins (> 95%) were analyzed by 10% SDS-PAGE.

Western blot. The purified His_6-DlaT protein was digested with factor Xa (New England BioLabs, MA) in reaction buffer (20 mM Tris-HCl, 100 mM NaCl, 2 mM $CaCl_2$, pH 7.4) for 18 hr at room temperature, and the untagged DlaT protein was used to immunize BALB/c mice (n=5). The DlaT polyclonal antibodies were used for Western blot analysis, as described previously (13).

Measurement of bacterial growth rate. Exponential growth rate of P. UF1 and its derivative strains were measured in MRS-lactate medium without antibiotics. The bacteria were first grown for 48 hr in MRS-lactate medium with corresponding antibiotics. Bacterial cultures (100 μL) were then inoculated into 10 mL fresh MRS-lactate medium without antibiotics and grown anaerobically at 30°C to an OD_{600} of 2.0. Every 6 hr, the bacterial cultures were diluted and plated on the MRS-lactate plates without antibiotics, and the bacterial growth rate was determined based on the number of colony-forming units (CFU) at different time points.

Monoassociation of GF mice with P. UF1 strains. C57BL/6 germfree (GF) mice (6-8 weeks) were provided by the Animal Care Facility of the University of Florida and maintained there until the experiments were performed (14, 15). C57BL/6 GF mice were gavaged with P. UF1 strains four times (4x) every 3 days, and the immune responses analyzed on day 14. Mice received P. UF1 (10^9 CFU/100 μL PBS) or its derivative strains (10^9 CFU/100 μL PBS),

including Δ*dlaT* P. UF1, P. UF1-1, P. UF1-2, P. UF1-3, S-layer$^-$ P. UF1, or *E. coli* JM109 (Promega, Madison, WI).

Generation of Δ*actA L. m* secreting the three DlaT peptides. The nucleotide sequence corresponding to the three DlaT peptides was synthesized and amplified with primers, 3Pep-F2/3Pep-R2. To use Δ*actA L. m* that is incapable of cell-to-cell spread by preventing bacterial-mediated host actin polymerization, we first employed standard allelic replacement methods to generate murinized Internalin A (InlA^m) in the background of a Δ*actA L. m*, followed by introduction of pIMK2-3pep (16) by electroporation (17, 18). To confirm that *L. m* strains InlA^{m}Δ*actA*, harboring a stably integrated pIMK2-3pep, were capable of expressing and secreting the recombinant DlaT peptides, an additional pIMK2-3pep construct containing a 6x-Histidine tag at the C-terminus (plasmid pIMK2-3pep-6xHis) was generated for detection. The supernatants of the bacterial cultures were collected, precipitated with 10% trichloroacetic acid, washed with 1 mL of 100% ethanol, and dissolved in SDS sample buffer. The protein samples were run on an 18% SDS-PAGE gel, transferred to a PVDF membrane, and detected by Western blot using an anti-His_6 mouse monoclonal antibody (Abcam, Cambridge, MA).

Bacterial infections. Mice were gavaged with either P. UF1, Δ*dlaT* P. UF1 or PBS on days -7, -4, -1, and 2 for Δ*actA L. m* relative to the infection. Mice were denied food, but given unrestricted access to water 8 hr prior to infection. The Δ*actA L. m* inoculum was suspended in 100 µL PBS with $CaCO_3$ (50 mg/ml). Mice were orally infected with Δ*actA L. m* (10^9 CFU/mouse) on day 0. Mice were then monitored daily and sacrificed on day 7. Fecal samples were collected on days 2, 4, and 7. Subsequently, the supernatants were diluted and plated on

BHI agar (200 μg/mL streptomycin). Colonies were counted at 37°C after 24-36 hr of growth. For experiments using *Foxp3*^{DTR} mice, mice were injected with diphtheria toxin (DT, 25 μg/kg body weight, i.p.) (Sigma-Aldrich, St. Louis, MO) on days -7, -6, -1 and 0.

Cell suspensions. Intestinal cells were isolated, as previously described (3). Enriched splenic cells were prepared by depleting B cells using plates coated with anti-mouse IgG (H+L) (Jackson ImmunoResearch Laboratories, Inc., West Grove, PA) for 30 min at 37°C. The non-adherent cells were subjected to CD4$^+$ T cell Isolation Kit II (MACS, Miltenyi Biotec, San Diego, CA). The purity of sorted cells analyzed by a LSR II Fortessa flow cytometer was determined to be > 98%. Subsequently, sorted cells were injected intraperitoneally (i.p.) into the *H2-Ab1*$^{-/-}$ recipient mice (10^6 cells/mouse).

Flow cytometry. Flow cytometric analysis was performed, as previously described (1). Briefly, isolated cells were stimulated with phorbol 12-myristate 13-acetate (PMA) (50 ng/mL) and ionomycin (2.5 μg/mL) in the presence of brefeldin A (Sigma-Aldrich, St. Louis, MO) at 37°C. Cell surface staining was carried out in PBS with 0.1% BSA, 1 mM EDTA, and 0.01% sodium azide. For live cell analyses, dead cells were excluded by staining with LIVE/DEAD® Fixable Blue Dead Cell Stain Kit (Molecular Probes, Thermo Fisher Scientific, Waltham, MA). Cells were incubated with Mouse Fc Blocking Reagent (Miltenyi Biotec, Auburn, CA) prior to staining. Cells were first stained for cell-surface markers and then resuspended in fixation/permeabilization solution [Cytofix/Cytoperm kit (BD Biosciences, San Jose, CA) or FOXP3 Fix/Perm buffer set (Biolegend, San Diego, CA) for FoxP3 intracellular staining)]. Intracellular staining was carried out in accordance with the manufacturer's instructions. Data

were collected by a LSR II Fortessa (BD Biosciences, San Jose, CA) and analyzed with FlowJo software (TreeStar, Ashland, OR). Antibodies for staining were purchased from BD Bioscience (San Jose, CA), Biolegend, eBioscience (San Diego, CA) or R&D Systems (Minneapolis, MN). The following antibodies or their corresponding isotype controls were used: CD45 (30-F11, Cat # 86-0451-42), CD11c (N418, Cat # 117338), CD11b (M1/70, Cat # 101212), F4/80 (BM8, Cat # 123112), GR1 (RB6-8C5, Cat # 108422), I-A/I-E MHCII (2G9, Cat # 558593), CD3 (145-2C11, Cat # 100330), CD4 (RM4-5, Cat # 100548), CD8 (53-6.7, Cat # 15-0081-83), CD45RB (C363.16A, Cat # 11-0455-85), CD25 (PC61.5, Cat # 56-0251-82), Thy1.1 (OX-7, Cat # 202535), Thy1.2 (30-H12, Cat # 105320), Pro-IL-1β (NJTEN3, Cat # 25-7114-82)/ isotype Rat IgG1, κ (Cat # 25-4301-82), IFNγ (XMG1.2, Cat # 505826)/ isotype Rat IgG1, κ (Cat # 400416), IL-17A (TC11-18H10.1, Cat # 506904 or 506922)/ isotype Rat IgG1, κ (Cat # 400408 or 400415), IL-10 (JES5-16E3, Cat # 505006, 563277 or 505031)/ isotype Rat IgG2b, κ (Cat # 400606, 562951 or 400649), FoxP3 (FJK-16A, Cat # 48-5773-82)/ isotype Rat IgG2a, κ (Cat # 48-4321-82), RORγt (AFKJS-9, Cat # 12-6988-80)/ isotype Rat IgG2a, κ (Cat # 12-4321-82), RORγt (BD2, Cat # 61-6981-82)/ isotype Rat IgG2a, κ (Cat # 61-4301-80), TGF-β (TW7-16B4, Cat # 141406 or 141410)/ isotype Rat IgG1 (Cat # 400120 or 400112), κ, IL-12/IL-23(p40) (C15.6, Cat # 561456)/ isotype Rat IgG1, κ (Cat # 560536), IL-6 (MP5-20F3, Cat # 11-7061-80)/ isotype Rat IgG1, κ (Cat # 11-4301-85), SIGNR1 (CD209b) (22D1, Cat # 17-2093-82)/ isotype Hamster IgG (Cat # 17-4888-81), IL-23R (Cat # FAB16861N/ isotype Rat IgG_1 (Cat # IC005N), IL-22 (poly5164, Cat # 516406)/ isotype Goat IgG (Cat # 403006). After dead and doublet cell exclusion and the subsequent $CD45^+$ and FCS/SSC selection, DCs were defined as $CD11c^+$ MHC II^{hi} $CD11b^+$ $F4/80^-$ (Supplemental Figure 11) and T cells as $CD3^+$ $CD4^+$ $CD8^-$ (Supplemental Figure 12). $IL\text{-}17A^+$ $IL\text{-}10^+$ $CD4^+$, $IL\text{-}17A^+$ $IFN\gamma^+$ $CD4^+$ or $IL\text{-}17A^+$ $IL\text{-}22^+$ $CD4^+$

cells were then plotted. Plotted Tregs were defined as IL-10^+ TGF-β^+ $CD3^+$ $CD4^+$ $CD8^-$ $FoxP3^+$ cells (Supplemental Figure 12). ILC3s were defined and plotted as $CD3^-$ $ROR\gamma t^+$ IL-22^+ IL-$17A^+$ cells (19) (Supplemental Figure 13).

DC-T cell co-cultures. Bone marrow DCs (BMDCs) were cultured, as previously described (20). BMDCs were pulsed with specific DlaT peptides (20 μg/mL) or S-layer (10 μg/ml), as a control, for 12 hr. For proliferation assays, $CD4^+$ T cells were labeled with 10 μM carboxyfluorescein succinimidyl ester (CFSE), according to the manufacturer's instructions (Molecular Probes, Waltham, MA), and co-cultured with peptide pulsed BMDCs. Each *in vitro* experiment was conducted in triplicates with splenic $CD4^+$ T cells pooled from three C57BL/6 mice gavaged with P. UF1 (10^9 CFU/mouse) four times. BMDCs (5×10^4) were co-cultured with $CD4^+$ T cells (1:10 ratio) for 5 days. Cells were stained with a panel of antibodies and analyzed by a LSR II Fortessa flow cytometer.

Tetramer analyses. The NIH Tetramer Core Facility at Emory University (Emory University Vaccine Center, Atlanta, GA) custom prepared MHCII tetramers presenting DlaT and control peptides. The following PE-labeled tetramers were generated: I-A(b) DlaT 208-222 (VGSSVPAAPAAAPAA), I-A(b) DlaT 245-259 (VAPPAPVAPSAPVAA), I-A(b) DlaT 109-123 (AAAPVAPPAPPAPAA), and a control tetramer (PVSKMRMATPLLMQA). MLN, splenic, and colonic cells from mice gavaged with P. UF1 were stained with I-A(b) DlaT 245-259 (VAPPAPVAPSAPVAA) (Tetramer $DlaT^{245}$ showed significant binding to MHCII) for 1 hr at 37°C. For MLN and splenic cells, a magnetic enrichment step was performed, as previously

described (21). Cells were labeled with extracellular antibodies and then treated with fixation/permeabilization buffer (Biolegend, San Diego, CA) for intracellular staining.

Adoptive transfer of naïve Thy1.1$^+$ CD4$^+$ CD25$^-$ CD45RB^{hi} T cells into Thy1.2$^+$ *Rag1*$^{-/-}$ mice. Splenic and LN Thy1.1$^+$ CD4$^+$ T cells were first magnetically enriched (Miltenyi Biotec, Auburn, CA) (1, 20). Enriched Thy1.1$^+$ CD4$^+$ CD25$^-$ CD45RB^{hi} were then sorted by a Sony cell sorter (SH800S Sony Biotechnology Inc., San Jose, CA) and subsequently passively transferred into Thy1.2$^+$ *Rag1*$^{-/-}$ mice (n=8, 6 weeks old) by retro orbital injections (5 x10^5 cells/mouse). Thy1.2$^+$ *Rag1*$^{-/-}$ mice were then gavaged with P. UF1 or PBS four times every three days. Twelve days later these groups of mice were sacrificed to analyze the differentiation of naive Thy1.1$^+$ CD4$^+$ CD25$^-$ CD45RB^{hi} T cells into Th17 cells by flow cytometry.

SIGNR1-hFC binding assay. SIGNR1, SIGNR3, and a control peptide were fused to the human Fc (hFc) portion of human IgG1 (SIGNR1-hFc; SIGNR3-hFc; Ctrl-hFc), as previously described (22). The cDNA of exons 4-10 encoding the extracellular domain (amino acid residues Val75-Gly325) of SIGNR1 (CD209b) (GenBank accession number NM_026972) was generated using total RNA isolated from intestinal tissue samples of C57BL/6 mice, and amplified using *Signr1*exp-F/*Signr1*exp-R primers. The product was fused in frame to the Fc region of human IgG1 by cloning into EcoRI and NcoI sites of the plasmid, pINFUSE-hIgG1-Fc2 (InvivoGen, San Diego, CA). Chinese hamster ovary (CHO) cells were transfected by a plasmid containing SIGNR1, and supernatants were collected two days later. The fusion proteins were purified using protein G columns (Thermo Fisher Scientific, Waltham, MA), according to the manufacturer's protocol. Purified SIGNR1–hFc and SIGNR3-hFc fusion proteins were confirmed by Western

blot using anti-SIGNR1 and anti-SIGNR3 antibodies (R&D Systems, Minneapolis, MN). Protein G column purified proteins were used for binding to P. UF1 or purified DlaT protein, as described previously (1). Bacterial samples (5 x10^6 bacteria) were blocked with 5% BSA at room temperature (RT) for 2 hr, followed by an incubation with 1 μg/ml SIGNR1-hFc protein in lectin buffer (50 mM Hepes, 5 mM $MgCl_2$, 5 mM $CaCl_2$, pH 7.4) with 0.5% BSA at RT for 2 hr. After three additional wash steps with lectin buffer, samples were incubated with PE-conjugated goat anti-human Fc antibody (Biolegend, San Diego, CA) at RT for 1 hr. Carbohydrate-binding specificity was analyzed by preincubation of SIGNR1-hFc with zymosan (20 μg/ml) (Sigma Aldrich, St. Louis, MO) at RT for 1 hr. Samples were washed three times with lectin buffer and analyzed by flow cytometry.

Gut transient colonization of P. UF1. C57BL/6 mice were gavaged one time (single oral gavage) with P. UF1, Δ*dlaT* P. UF1 (10^9 CFU/mouse) or PBS. Every day, mice (n=2-3/group) were sacrificed to collect cecal and fecal samples. GF mice were monoassociated with a single oral gavage with P. UF1 (10^9 CFU/mouse) and fecal samples were collected daily (n=5). Bacterial genomic DNA was isolated using a Zymo Fecal DNA MiniPrep kit (Zymo Research, Irvine, CA). To quantify the bacterial strains in the fecal and cecal contents, fecal DNA (10 ng) was added to SsoAdvanced SYBR Green Supermix (Bio-Rad) containing either P. UF1-specific primers, P3/P4, or 16S rDNA universal primers, rDNA-F/rDNA-R. The percentage of P. UF1 or Δ*dlaT* P. UF1 in total bacteria was expressed as the percentage of *dlaT* copies normalized to the copies of 16S rDNA. To quantify P. UF1 in the fecal samples of GF mice, plasmid pYMZ-P4-*dlaT* was used to generate the standard curve of *dlaT* using P3/P4 primers. The colonization of P. UF1 in GF mice was expressed as the copy number of *dlaT* gene per milligram (mg) of fecal

samples. Statistical analyses were performed by unpaired *t*-test comparing the different days to day 0.

Bacterial transcriptomic analyses. Total RNA was extracted from P. UF1 and Δ*dlaT* P. UF1 strains (3 replicates of each strain), and DNA contaminants were removed by an Ambion TURBO DNA-free kit (Thermo Fisher Scientific, Waltham, MA). The ScriptSeq Complete Gold Kit (Illumina, Inc., San Diego, CA) was used for rRNA depletion and the cDNA library generation (23, 24). Subsequently, cDNA libraries were evaluated, pooled, and sequenced on the Illumina MiSeq, which generates 7-8 million paired-end reads/sample (~75 nt). The sequence reads first underwent data preprocessing and quality evaluation, including trimming off the low quality ends of reads. Rockhopper was used to map sequence reads to the annotated P. UF1 genome to normalize the counts values by upper quartile normalization, and to perform differential expression analyses using the negative binomial (NB) statistical model (25). Principal component analyses (PCA) were performed based on normalized counts to visualize the separation between groups using Python. Selected genes were visualized in a heatmap after Z-score transformation upon normalized counts across all samples in each gene (filtered by $P < 0.05$, NB model; fold change > 1.5). Diagrams of gene expression associated with the tricarboxylic acid (TCA) cycle and pyruvate metabolism were depicted. The RNA-seq data were submitted to the NCBI gene expression omnibus (GEO, accession number GSE89528).

Ultra-high resolution metabolomic analyses. Mouse fecal samples and P. UF1 cultures were collected and analyzed (26-30). The samples were processed by acetonitrile (2:1, v/v), followed by centrifugation, before being analyzed by a high-resolution mass spectrometer coupled with

liquid chromatography (LC-MS) (26, 28). The fecal samples were analyzed on a LTQ-FTICR mass spectrometer and the bacterial samples on an Orbitrap Fusion Tribrid Mass Spectrometer (Thermo Fisher, San Diego, CA). Each sample was added spike-in controls and run in triplicates; standard reference samples were run in the beginning and end of each batch. An in-house informatics pipeline was used to perform peak detection, noise filtering, mass to charge (*m/z*) ratio and retention time alignment, and feature quantification (27, 29, 30). Subsequently, the feature table was subjected to quality assessment, including exclusion of data for technical replicates with overall Pearson correlation (r) < 0.70. Feature values (MS peak intensities) of each sample were summarized by the average of filtered non-zero technical replicates, normalized by total ion intensity, and log2 transformed. For each experiment, PCA were performed on all metabolomic features to visualize the separation between groups using Python. Significant metabolomic features were selected by *t*-test or ANOVA, and subjected to pathway analyses with the Mummichog software (27). In pathway analyses of fecal samples from control GF mice treated with PBS *versus* GF mice monoassociated with P. UF1, 363 significant metabolomic features ($P < 0.05$, *t*-test) were used as Mummichog input. In the analyses of bacterial samples from P. UF1 *versus* Δ*dlaT* P. UF1, 389 significant metabolomic features ($P < 0.005$, *t*-test) were used as Mummichog input. In pathway analyses of fecal samples from P. UF1-gavaged *H2-Ab1*$^{-/-}$ mice with transferred T cells *versus* those from PBS-gavaged *H2-Ab1*$^{-/-}$ mice with transferred T cells, 509 significant metabolomic features ($P < 0.005$, *t*-test) were used as Mummichog input. In pathway analyses of fecal samples from P. UF1: P. UF1-1 joint group *versus* Δ*dlaT* P. UF1: P. UF1-2 joint group, 427 significant features ($P < 0.0001$, *t*-test) were used as Mummichog input. In pathway analyses of fecal samples from either *Signr1*$^{+/+}$ or *Signr1*$^{-/-}$ mice infected with Δ*actA L. m* only, Δ*actA L. m* + P. UF1, Δ*actA L. m* + Δ*dlaT* P. UF1 or

Δ*actA L. m*^{3pep}, respectively, 326 ($P < 0.005$) or 631 ($P < 0.05$) significant features were used for Mummichog input, respectively. Only adduct ions with $[M+H]^+$ and $[M+Na]^+$ were chosen for visualization in a heatmap with Z-score transformed values presented. Among the metabolites, arginine, citrulline, betaine/valine, tryptophan, phenylalanine, methionine, lysine, aspartate, tyrosine and creatine were confirmed by chemical standards, while others were based on high-confidence database matches (< 10 ppm).

Supplemental References:

1. Lightfoot, Y.L., Selle, K., Yang, T., Goh, Y.J., Sahay, B., Zadeh, M., Owen, J.L., Colliou, N., Li, E., Johannssen, T., et al. 2015. SIGNR3-dependent immune regulation by Lactobacillus acidophilus surface layer protein A in colitis. *EMBO J* 34:881-895.
2. Yang, T., Santisteban, M.M., Rodriguez, V., Li, E., Ahmari, N., Carvajal, J.M., Zadeh, M., Gong, M., Qi, Y., Zubcevic, J., et al. 2015. Gut dysbiosis is linked to hypertension. *Hypertension* 65:1331-1340.
3. Lightfoot, Y.L., Yang, T., Sahay, B., Zadeh, M., Cheng, S.X., Wang, G.P., Owen, J.L., and Mohamadzadeh, M. 2014. Colonic immune suppression, barrier dysfunction, and dysbiosis by gastrointestinal bacillus anthracis Infection. *PLoS One* 9:e100532.
4. Bokulich, N.A., Subramanian, S., Faith, J.J., Gevers, D., Gordon, J.I., Knight, R., Mills, D.A., and Caporaso, J.G. 2013. Quality-filtering vastly improves diversity estimates from Illumina amplicon sequencing. *Nat Methods* 10:57-59.
5. Rideout, J.R., He, Y., Navas-Molina, J.A., Walters, W.A., Ursell, L.K., Gibbons, S.M., Chase, J., McDonald, D., Gonzalez, A., Robbins-Pianka, A., et al. 2014. Subsampled open-reference clustering creates consistent, comprehensive OTU definitions and scales to billions of sequences. *PeerJ* 2:e545.
6. McDonald, D., Price, M.N., Goodrich, J., Nawrocki, E.P., DeSantis, T.Z., Probst, A., Andersen, G.L., Knight, R., and Hugenholtz, P. 2012. An improved Greengenes taxonomy with explicit ranks for ecological and evolutionary analyses of bacteria and archaea. *ISME J* 6:610-618.
7. Segata, N., Izard, J., Waldron, L., Gevers, D., Miropolsky, L., Garrett, W.S., and Huttenhower, C. 2011. Metagenomic biomarker discovery and explanation. *Genome Biol* 12:R60.
8. Asnicar, F., Weingart, G., Tickle, T.L., Huttenhower, C., and Segata, N. 2015. Compact graphical representation of phylogenetic data and metadata with GraPhlAn. *PeerJ* 3:e1029.
9. Brede, D.A., Faye, T., Stierli, M.P., Dasen, G., Theiler, A., Nes, I.F., Meile, L., and Holo, H. 2005. Heterologous production of antimicrobial peptides in *Propionibacterium freudenreichii*. *Appl Environ Microbiol* 71:8077-8084.

10. Monera, O.D., Kay, C.M., and Hodges, R.S. 1994. Protein denaturation with guanidine hydrochloride or urea provides a different estimate of stability depending on the contributions of electrostatic interactions. *Protein Sci* 3:1984-1991.

11. Deutsch, S.M., Parayre, S., Bouchoux, A., Guyomarc'h, F., Dewulf, J., Dols-Lafargue, M., Bagliniere, F., Cousin, F.J., Falentin, H., Jan, G., et al. 2012. Contribution of surface beta-glucan polysaccharide to physicochemical and immunomodulatory properties of Propionibacterium freudenreichii. *Appl Environ Microbiol* 78:1765-1775.

12. Kiatpapan, P., Hashimoto, Y., Nakamura, H., Piao, Y.Z., Ono, H., Yamashita, M., and Murooka, Y. 2000. Characterization of pRGO1, a plasmid from Propionibacterium acidipropionici, and its use for development of a host-vector system in propionibacteria. *Appl Environ Microbiol* 66:4688-4695.

13. Sahay, B., Ge, Y., Colliou, N., Zadeh, M., Weiner, C., Mila, A., Owen, J.L., and Mohamadzadeh, M. 2015. Advancing the use of Lactobacillus acidophilus surface layer protein A for the treatment of intestinal disorders in humans. *Gut Microbes* 6:392-397.

14. Ahern, P.P., Faith, J.J., and Gordon, J.I. 2014. Mining the human gut microbiota for effector strains that shape the immune system. *Immunity* 40:815-823.

15. Faith, J.J., Ahern, P.P., Ridaura, V.K., Cheng, J., and Gordon, J.I. 2014. Identifying gut microbe-host phenotype relationships using combinatorial communities in gnotobiotic mice. *Sci Transl Med* 6:220ra211.

16. Monk, I.R., Gahan, C.G., and Hill, C. 2008. Tools for functional postgenomic analysis of listeria monocytogenes. *Appl Environ Microbiol* 74:3921-3934.

17. Park, S.F., and Stewart, G.S. 1990. High-efficiency transformation of Listeria monocytogenes by electroporation of penicillin-treated cells. *Gene* 94:129-132.

18. Wollert, T., Pasche, B., Rochon, M., Deppenmeier, S., van den Heuvel, J., Gruber, A.D., Heinz, D.W., Lengeling, A., and Schubert, W.D. 2007. Extending the host range of Listeria monocytogenes by rational protein design. *Cell* 129:891-902.

19. Li, S., Heller, J.J., Bostick, J.W., Lee, A., Schjerven, H., Kastner, P., Chan, S., Chen, Z.E., and Zhou, L. 2016. Ikaros Inhibits Group 3 Innate Lymphoid Cell Development and Function by Suppressing the Aryl Hydrocarbon Receptor Pathway. *Immunity* 45:185-197.

20. Mohamadzadeh, M., Pfeiler, E.A., Brown, J.B., Zadeh, M., Gramarossa, M., Managlia, E., Bere, P., Sarraj, B., Khan, M.W., Pakanati, K.C., et al. 2011. Regulation of induced colonic inflammation by Lactobacillus acidophilus deficient in lipoteichoic acid. *Proc Natl Acad Sci U S A* 108 Suppl 1:4623-4630.

21. Moon, J.J., Chu, H.H., Pepper, M., McSorley, S.J., Jameson, S.C., Kedl, R.M., and Jenkins, M.K. 2007. Naive CD4(+) T cell frequency varies for different epitopes and predicts repertoire diversity and response magnitude. *Immunity* 27:203-213.

22. Eriksson, M., Johannssen, T., von Smolinski, D., Gruber, A.D., Seeberger, P.H., and Lepenies, B. 2013. The C-Type Lectin Receptor SIGNR3 Binds to Fungi Present in Commensal Microbiota and Influences Immune Regulation in Experimental Colitis. *Front Immunol* 4:196.

23. Giannoukos, G., Ciulla, D.M., Huang, K., Haas, B.J., Izard, J., Levin, J.Z., Livny, J., Earl, A.M., Gevers, D., Ward, D.V., et al. 2012. Efficient and robust RNA-seq process for cultured bacteria and complex community transcriptomes. *Genome biology* 13:R23.

24. Alberti, A., Belser, C., Engelen, S., Bertrand, L., Orvain, C., Brinas, L., Cruaud, C., Giraut, L., Da Silva, C., Firmo, C., et al. 2014. Comparison of library preparation methods reveals their impact on interpretation of metatranscriptomic data. *BMC genomics* 15:912.

25. McClure, R., Balasubramanian, D., Sun, Y., Bobrovskyy, M., Sumby, P., Genco, C.A., Vanderpool, C.K., and Tjaden, B. 2013. Computational analysis of bacterial RNA-Seq data. *Nucleic Acids Res* 41:e140.

26. Frediani, J.K., Jones, D.P., Tukvadze, N., Uppal, K., Sanikidze, E., Kipiani, M., Tran, V.T., Hebbar, G., Walker, D.I., Kempker, R.R., et al. 2014. Plasma metabolomics in human pulmonary tuberculosis disease: a pilot study. *PLoS One* 9:e108854.

27. Li, S., Park, Y., Duraisingham, S., Strobel, F.H., Khan, N., Soltow, Q.A., Jones, D.P., and Pulendran, B. 2013. Predicting network activity from high throughput metabolomics. *PLoS Comput Biol* 9:e1003123.

28. Neujahr, D.C., Uppal, K., Force, S.D., Fernandez, F., Lawrence, C., Pickens, A., Bag, R., Lockard, C., Kirk, A.D., Tran, V., et al. 2014. Bile acid aspiration associated with lung chemical profile linked to other biomarkers of injury after lung transplantation. *Am J Transplant* 14:841-848.

29. Uppal, K., Soltow, Q.A., Strobel, F.H., Pittard, W.S., Gernert, K.M., Yu, T., and Jones, D.P. 2013. xMSanalyzer: automated pipeline for improved feature detection and downstream analysis of large-scale, non-targeted metabolomics data. *BMC Bioinformatics* 14:15.

30. Yu, T., Park, Y., Li, S., and Jones, D.P. 2013. Hybrid feature detection and information accumulation using high-resolution LC-MS metabolomics data. *J Proteome Res* 12:1419-1427.

Supplemental Tables

	Breast milk (n=20)	Formula (n=20)	*P* value
Gestational Age (weeks)	29 ± 2	30 ± 2	0.208[a]
Birth Weight (grams)	1198 ± 383	1360 ± 436	0.217[a]
Caucasian	80%	35%	<0.01[b]
Vaginal Delivery	25%	45%	0.3203[b]
Chorioamnionitis	20%	60%	<0.05[b]
Male	70%	50%	0.3332[b]
Maternal Antibiotics	90%	85%	1[b]
Infant Antibiotics	80%	85%	1[b]

Values represent mean ± SD, unless otherwise indicated. [a]Student's two-tailed t test; [b]Fisher's exact test.

Table S1. Selected preterm infant cohorts

Oligonucleotide	Sequence (5’ to 3’)
DlaT-F	CCCAAGCTTGAGGTGGCTGAAGGAAGTTG
DlaT-R	CCCGGATCCTCCTCCTTGACGTGGATCTC
CdlaT-F	CCCTCTAGACCAGCTTCTCGTGACACTCATTC
CdlaT-R	CCCGGATCCCGCGATCCCCGTTACGG
3Pep-lap-R	CGGCTGCGGGAATCGGCATGGTTCTACGTGACTCCTTTG
3Pep-lap-F	CAAAGGAGTCACGTAGAACCATGCCGATTCCCGCAGCCG
3Pep-R	CCCGGATCCCTAAGCCGGTGGGTTCACCG
Pep1-lap-F	CCCCGATTCCCGCAGCCGCGGCACCTGCCGGC
Pep1-lap-R	GCCGGCAGGTGCCGCGGCTGCGGGAATCGGGG
Pep2-lap-F	CCGTACTCGGCGTCGTCCCTGCGGCACCCGCC
Pep2-lap-R	GGCGGGTGCCGCAGGGACGACGCCGAGTACGG
Pep3-lap-F	GCGGCTCCGGCCCCCCCGCCCGCGGCGCCG
Pep3-lap-R	CGGCGCCGCGGGCGGGGGGGCCGGAGCCGC
3Pep-F2	CAACAAACTGAAGCAAAGGATGTTGGTAGTAGTGTCCCA
3Pep-R2	ATATGTCGACCTATGCAGC AACTGGTGCA
HlySS-F	ATATCCATGGCCAAAAAAATAATGCTAGTTTTTATTA
HlySS-R	TGGGACACTACTACCAACATCCTTTGCTTCAGTTTGTTG
Signr1exp-F	CCGGAATTCGCAAGTCTCCAAAACCCCA
Signr1exp-R	CATGCCATGGGGCCTTCAGTGCATGGGGTTGC
P1	GTCTTCTGCCCCATACGCTAA
P2	GATGTCCTCGGAGTCGTGGTA
P3	CACCCTGACGGAGATCCAC
P4	CCGACGACGCCGAGTAC
GroL2-F	CAATGTCGTGTTGGAGAAG
GroL2-R	CGCCGATCTTGTGGTAGG
Gapdh-F	GGTGAAGGTCGGTGTGAACG
Gapdh-R	CTCGCTCCTGGAAGATGGTG
Signr1-F	TTGATGGTCAGCGGCAGCAGG
Signr1-R	TCAGCAGGAGCCCAGCCAAGA
Signr3-F	GGGCCCAACTGGTCATCATA
Signr3-R	AGCGTGTAAAGCTGGGTGAC
rDNA-F	AGGATTAGATACCCTGGTA
rDNA-R	CRRCACGAGCTGACGAC
DlaT-F6	CCCGGTACCTCGACCGAAGTCACACTGCC
DlaT-R6	CCCGGATCCCCTACTGGTTCAGACCGAACTCAG
IL-1b-F	AAGGAGAACCAAGCAACGAC
IL-1b-R	GAGATTGAGCTGTCTGCTCA
IL-6-F	AAAGAGTTGTGCAATGGCAATTCT
IL-6-R	AAGTGCATCATCGTTGTTCATACA
IL-12p35-F	CACCCTTGCCCTCCTAAACC
IL-12p35-R	CTAAGACACCTGGCAGGTCCA
IL-23p19-F	AGGCTCCCCTTTGAAGATGT

IL-23p19-R	CCAGCGGGACATATGAATCT
IL-12/23p40-F	CCACTCACATCTGCTGCTCCACAA
IL-12/23p40-R	ACTTCTCATAGTCCCTTTGGTCCAG
iNOS-F	AACGGAGAACGTTGGATTTG
iNOS-R	CAGCACAAGGGGTTTTCTTC
Socs1-F	AGGATGGTAGCACGCAAC
Socs1-R	GAAGACGAGGACGAGGAG

Table S2. **Oligonucleotides used in this study**

Supplemental Figures

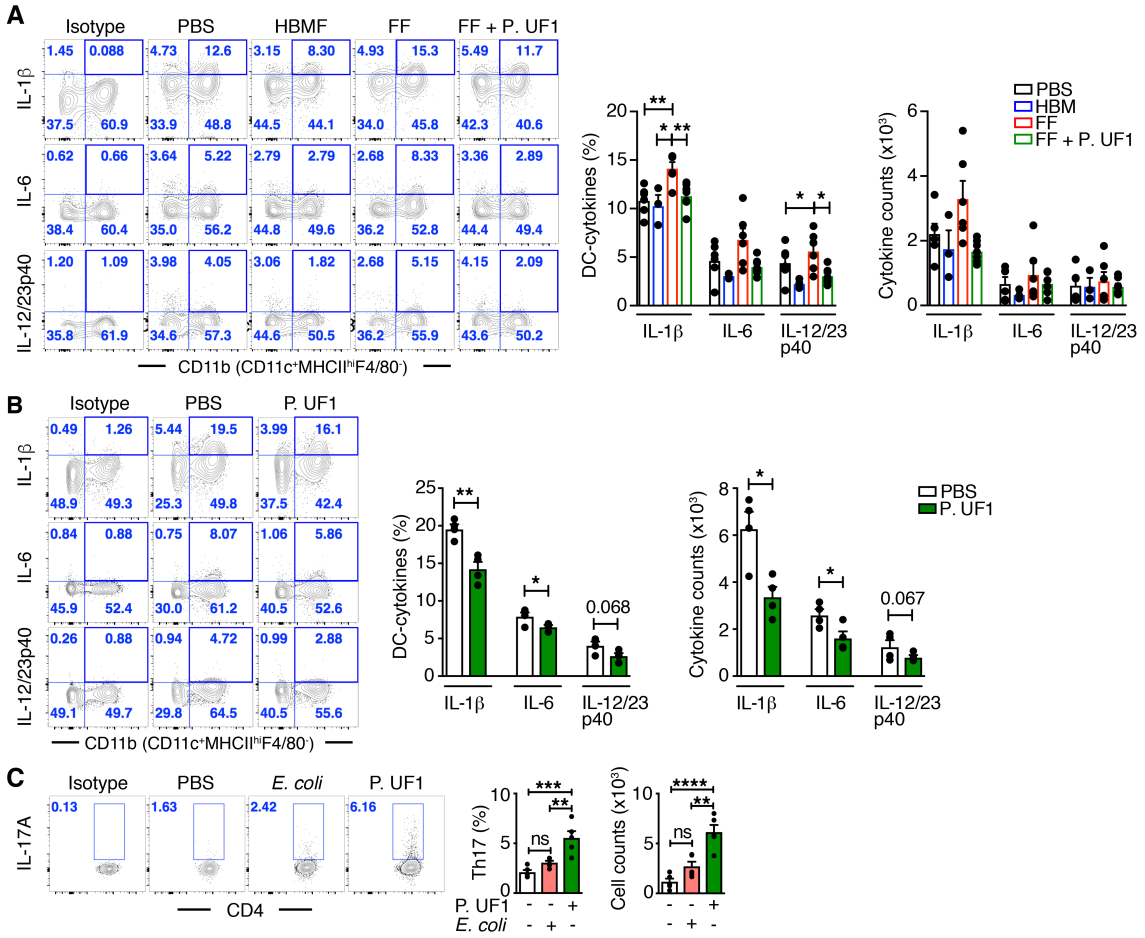

Supplemental Figure 1. Modulation of proinflammatory responses by HBMF-preterm infants' microbiota.

(**A**) Germfree (GF) mice were transfaunated with HBMF-preterm infants' microbiota (blue), FF-preterm infants' microbiota (red), FF-preterm infants' microbiota plus four treatments with P. UF1 (green) or left untransfaunated (black); colonic immune responses were analyzed two weeks later. Representative data of flow plots, percentage (%), and total cell counts of IL-1β^{+}, IL-6^{+} and IL-12/23p40^{+} DCs. (**B**) GF mice were monoassociated with P. UF1 (green) or gavaged with PBS (white), and induced colonic immune responses were analyzed. Representative data of flow plots, percentage (%), and total cell counts of IL-1β^{+}, IL-6^{+} and IL-12/23p40^{+} DCs. (**C**) GF mice were monoassociated with P. UF1 (green), *E. coli* JM109 (pink), or gavaged with PBS (white), and induced colonic Th17 response was analyzed. Representative data of flow plots, percentage (%), and total cell counts of Th17 cells. Data are pooled from 2 independent experiments (n=3-7 mice/group, **A**) or representative of 1 (n=5 mice/group, **C**) or 6 (n=4 mice/group, **B**) independent experiments. Error bars indicate the mean ± S.E.M. **P* < 0.05, ***P* < 0.01, ****P* < 0.001, *****P* < 0.0001, by ANOVA plus Tukey post-test (**A** and **C**) or two-tailed unpaired *t*-test (**B**).

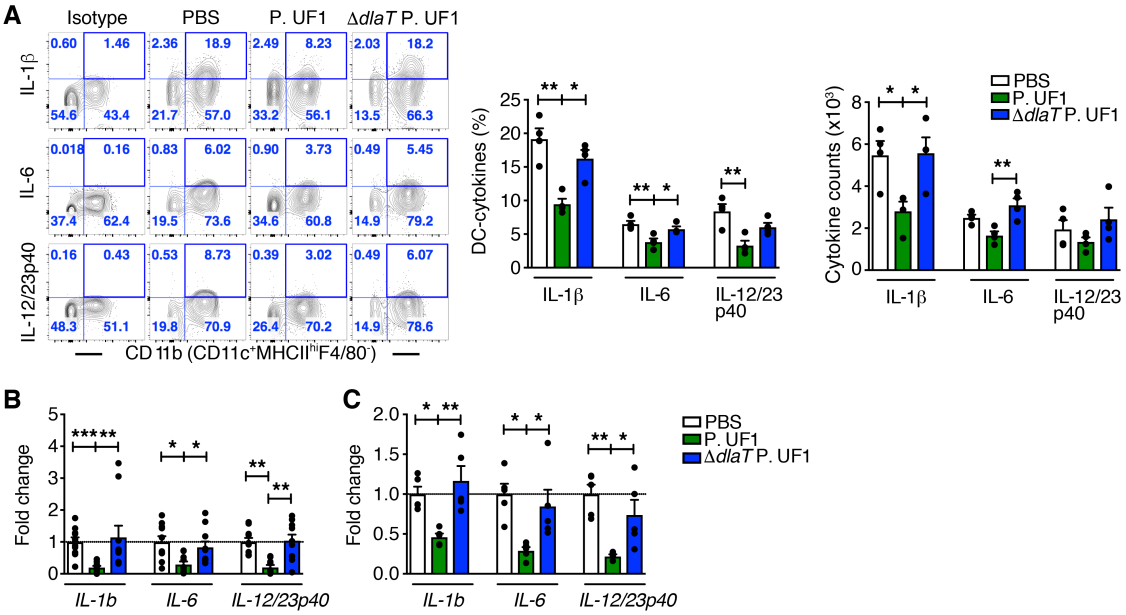

Supplemental Figure 2. Modulation of proinflammatory cytokines by P. UF1.

(**A**) GF mice were gavaged with P. UF1 (green), Δ*dlaT* P. UF1 (blue) or PBS (white). Colonic immune responses were analyzed two weeks later (n=4 mice/group). Representative data of flow plots, percentage (%), and total cell counts of IL-1β^{+}, IL-6^{+} and IL-12/23p40^{+} DCs. (**B**) RNA samples were isolated from colonic tissue of mice gavaged with P. UF1 (green), Δ*dlaT* P. UF1 (blue), or PBS (white). Cytokine expression (e.g., *IL-1b, IL-6, IL-12/23p40*) was analyzed by qRT-PCR. Data are represented as fold change over PBS (n=10 mice/group). (**C**) RNA samples were isolated from sorted colonic DCs of GF mice gavaged with P. UF1 (green), Δ*dlaT* P. UF1 (blue), or PBS (white). Cytokine expression (e.g., *IL-1b, IL-6, IL-12/23p40*) was analyzed by qRT-PCR. Data are represented as fold change over PBS (n=5 mice/group). Data are pooled from 3 independent experiments (**B**) or representative of 1 (**C**) or 3 (**A**) independent experiments. Error bars indicate the mean ± S.E.M. **P* < 0.05, ***P* < 0.01, ****P* < 0.001, by ANOVA plus Tukey post-test (**A** and **C**) or Kruskal-Wallis plus Dunn's post-test (**B**).

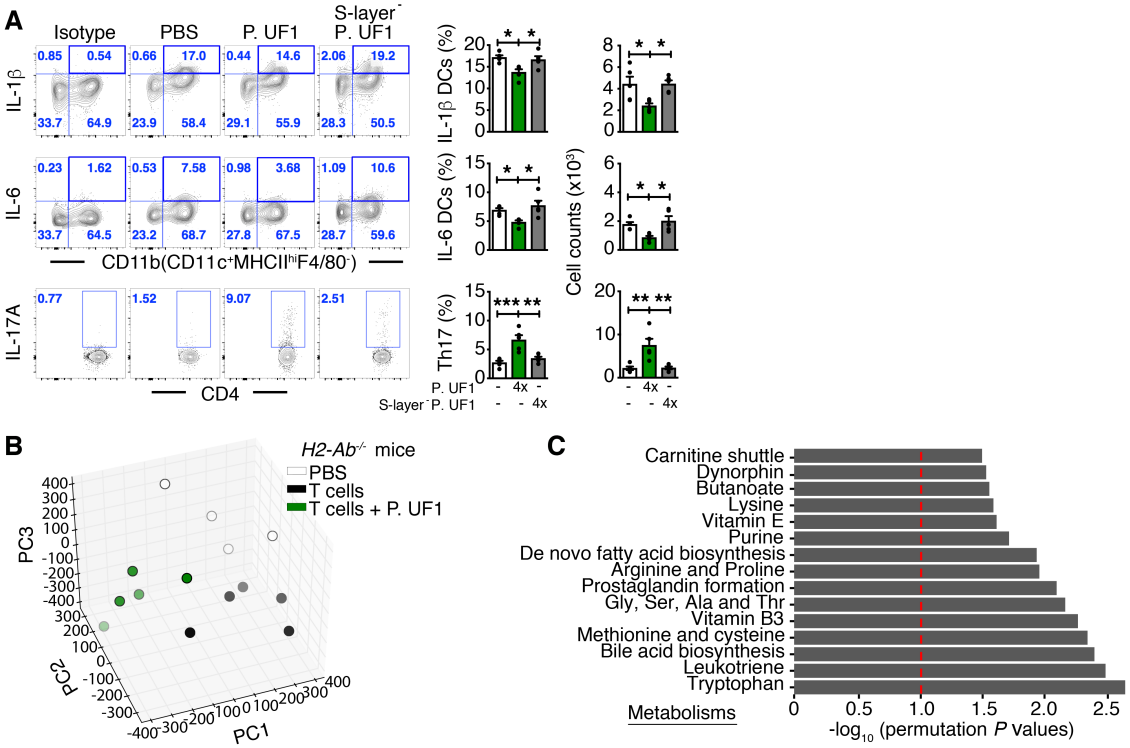

Supplemental Figure 3. Induction of Th17 cell differentiation by P. UF1.
(**A**) Representative data of flow plots, percentage (%), and total counts of DCs and Th17 cells in C57BL/6 mice gavaged with PBS, P. UF1 or S-layer^{-} P. UF1 (n=5 mice/group). (**B-C**) CD4^{+} splenic cells derived from C57BL/6 mice gavaged with P. UF1 were transferred into *H2-Ab1*$^{-/-}$ recipient mice. *H2-Ab1*$^{-/-}$ mice were gavaged 4 times (4x) with P. UF1 (10^{9} CFU/mouse), or with PBS (n=4-5 mice/group). Principal component (PC) (**B**) and metabolic pathway (**C**) analyses of fecal metabolites from *H2-Ab1*$^{-/-}$ mice transferred with CD4^{+} T cells *versus* with CD4^{+} T cells plus P. UF1 treatment. Red dashed lines show permutation $P = 0.05$. Data are representative of 2 (**A-C**) independent experiments. Error bars indicate the mean ± S.E.M. *$P < 0.05$, **$P < 0.01$, ***$P < 0.001$, by ANOVA plus Tukey post-test (**A**).

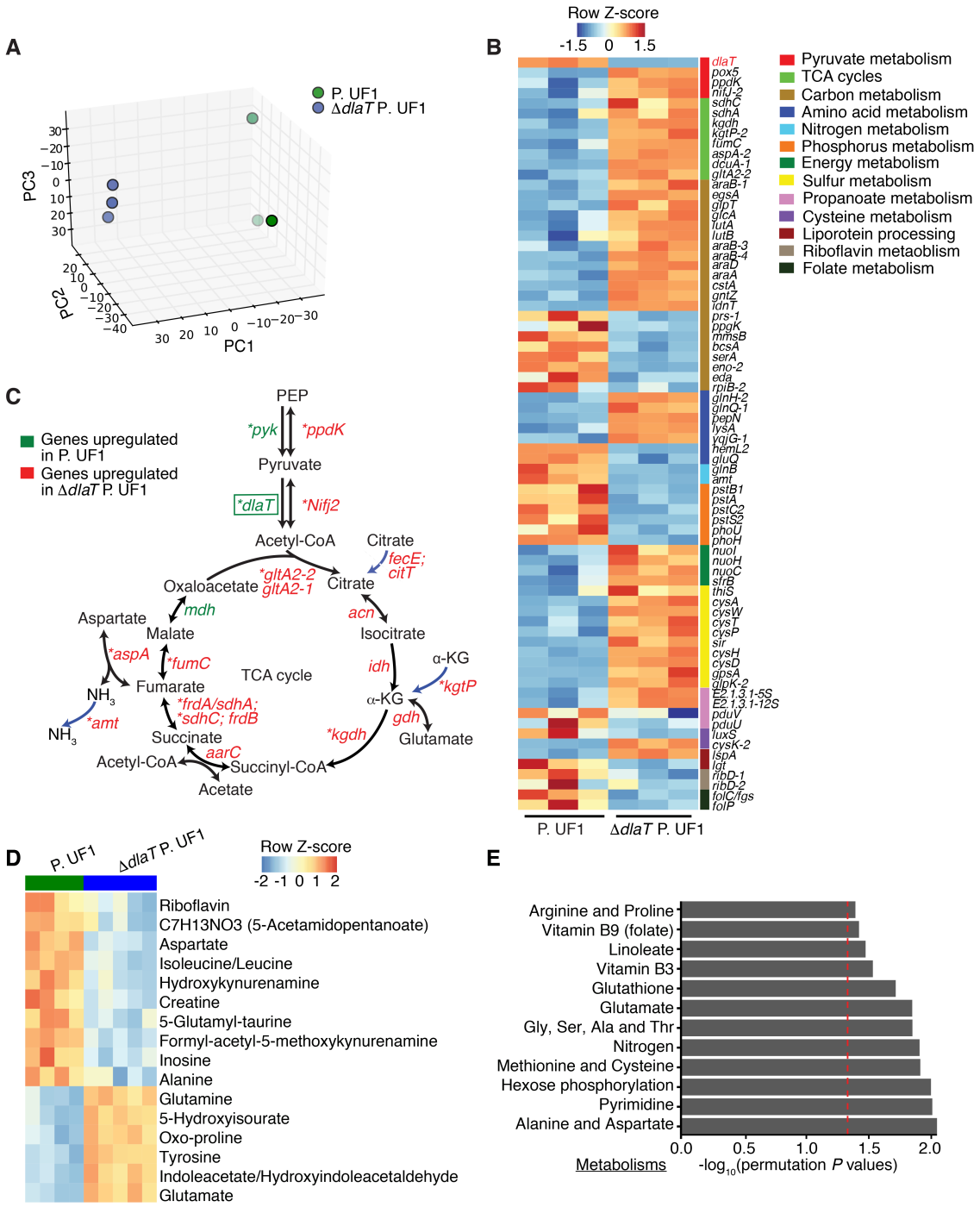

Supplemental Figure 4. Transcriptomic and Metabolomic profiling of P. UF1 and Δ*dlaT* P. UF1.

P. UF1 and Δ*dlaT* P. UF1 were grown anaerobically in MRS-lactate medium, and the bacterial pellets were subjected to transcriptomic and metabolomics analyses. (**A**) Principal component analysis (PCA) of transcriptomes of P. UF1 and Δ*dlaT* P. UF1. (**B**) Heatmap showing differential gene expression associated with indicated pathways in P. UF1 and Δ*dlaT* P. UF1 (filtered by $P < 0.05$, NB model, fold change > 1.5). (**C**) Diagram of gene expression associated with tricarboxylic acid (TCA) cycle and pyruvate metabolism. Genes significantly upregulated in

either condition ($P < 0.05$, NB model, fold change > 1.5) are indicated with asterisk (*). (**D**) Heatmap showing the differential abundance of selected metabolites in P. UF1 and Δ*dlaT* P. UF1. ($P < 0.005$, *t*-test). (**E**) Metabolic pathway analyses showing significant different pathways (permutation $P < 0.05$) between P. UF1 and Δ*dlaT* P. UF1 strains. Data are representative of 2 independent experiments (n=3 samples/group, **A-C**) or (n=4-5 samples, **D** and **E**).

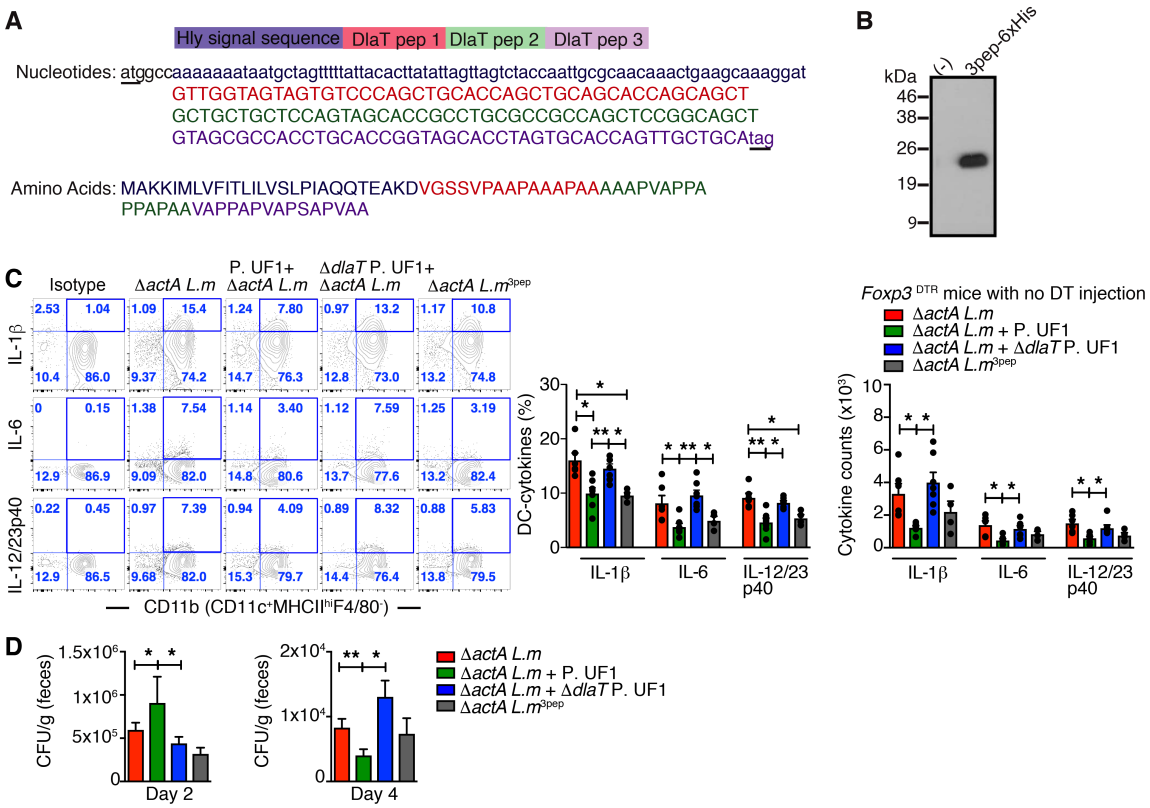

Supplemental Figure 5. Immune regulation by P. UF1 during Δ*actA L. m* infection.
(**A** and **B**) The nucleotides and amino acids of Hly signal sequence and the DlaT 3pep (**A**) were expressed by Δ*actA L. m* and protein secretion was confirmed by Western blot using anti-His_6 monoclonal antibody (**B**). (**C**) *Foxp3*^{DTR} mice with no diphtheria toxin (DT) injection were gavaged with PBS (red), P. UF1 (green) or with Δ*dlaT* P. UF1 (blue), and orally infected with Δ*actA L. m*. One group of mice was orally infected with Δ*actA L. m*^{3pep} (grey). Representative data of flow plots, percentage (%), and total cell counts of IL-1β^{+}, IL-6^{+} and IL-12/23p40^{+} DCs (n=4-7 mice/group). (**D**) Bacterial burden of Δ*actA L. m* in the fecal samples from mice (treated and infected as described in **C,** n=4-7 mice/group) collected two and four days post-infection. Data are pooled from 2 independent experiments (**C** and **D**). Error bars indicate the mean ± S.E.M. **P* < 0.05, ***P* < 0.01, by ANOVA plus Tukey post-test (**D**) or Kruskal-Wallis plus Dunn's post-test (**C**).

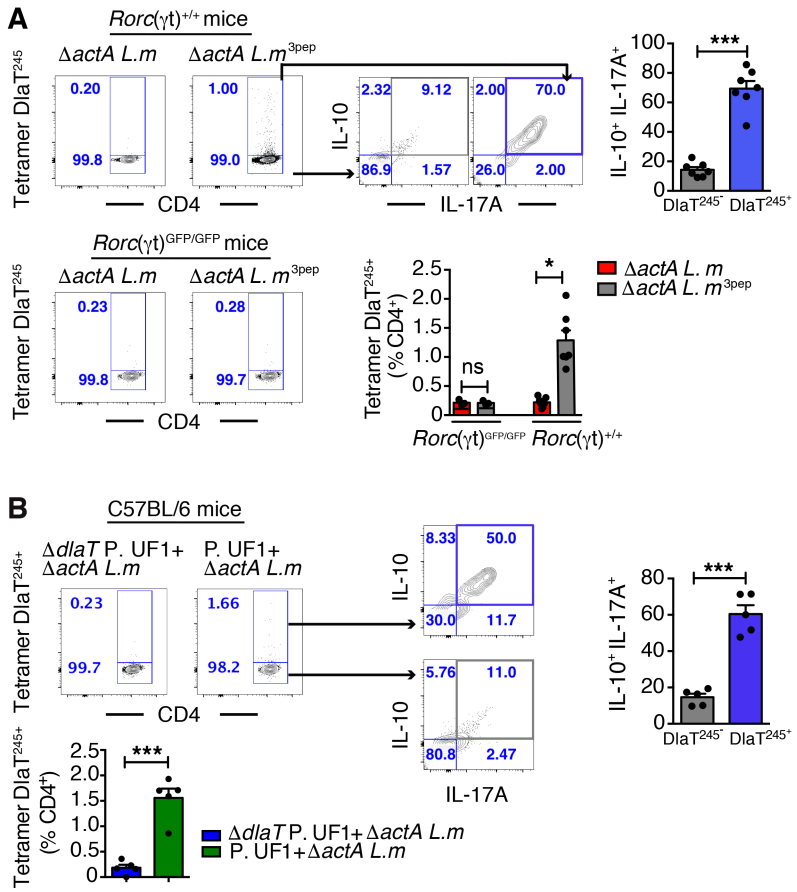

Supplemental Figure 6. Induction of DlaT-specific Th17 cells by P. UF1 during Δ*actA L. m* infection.

(**A**) *Rorc*(γt)$^{+/+}$ (n=7 mice/group) or *Rorc*(γt)$^{GFP/GFP}$ (n=3 mice/group) mice were orally infected with Δ*actA L. m* or Δ*actA L. m*^{3pep}. Analyses of tetramer DlaT^{245+} CD4^{+} T cells and their positivity for IL-17A and IL-10 in *Rorc*(γt)$^{+/+}$ or *Rorc*(γt)$^{GFP/GFP}$ mice orally infected with Δ*actA L. m*, or Δ*actA L. m*^{3pep}. (**B**) C57BL/6 mice (n=5 mice/group) were gavaged with P. UF1 (green) or with Δ*dlaT* P. UF1 (blue) and orally infected with Δ*actA L. m*. Analyses of tetramer DlaT^{245+} CD4^{+} T cells and their positivity for IL-17A and IL-10. Data are pooled from 2 independent experiments (**A** and **B**). Error bars indicate the mean ± S.E.M. Not significant (ns), *$P < 0.05$, **$P < 0.01$, ***$P < 0.001$, by two-tailed unpaired *t*-test (**A** and **B**).

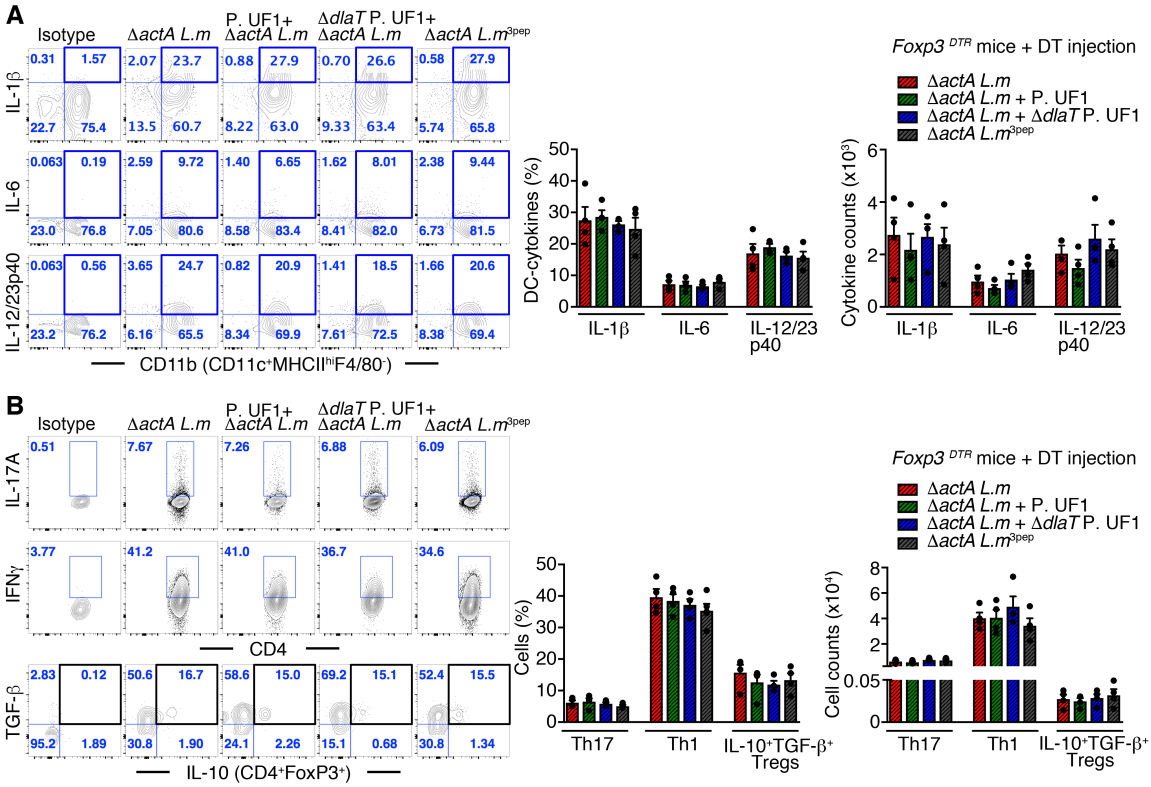

Supplemental Figure 7. Tregs depletion during Δ*actA L. m* infection.

Foxp3^{DTR} mice (n=4 mice/group) were intraperitoneally injected with diphtheria toxin (DT) (25 µg/kg body weight, i.p). Mice were then gavaged with PBS (red), P. UF1 (green), or with Δ*dlaT* P. UF1 (blue), and orally infected with Δ*actA L. m*. One group of mice was orally infected with Δ*actA L. m*^{3pep} (grey). Colonic immune responses were analyzed 7 days later. Representative data of flow plots, percentage (%), and total cell counts of IL-1β^{+}, IL-6^{+} and IL-12/23p40^{+} DCs (**A**) and representative data of flow plots, percentage (%), and total cell counts of colonic Th17 cells, Th1 cells and IL-10^{+} TGF-β^{+} FoxP3^{+} Tregs (**B**). Data are representative of 3 independent experiments. Error bars indicate the mean ± S.E.M. Statistical significance was determined by ANOVA plus Tukey post-test.

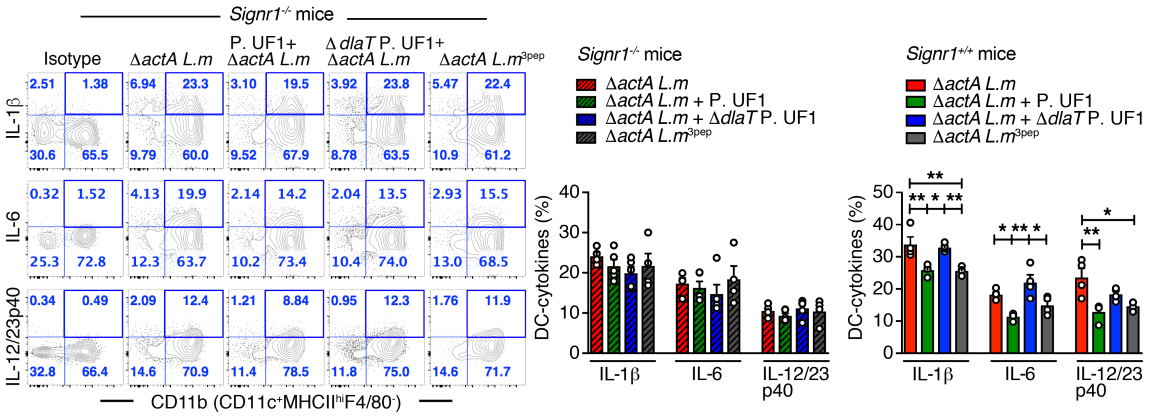

Supplemental Figure 8. SIGNR1 dependent regulation of intestinal immunity during Δ*actA L. m* infection.

Signr1$^{-/-}$ or *Signr1*$^{+/+}$ mice were gavaged with PBS (red), P. UF1 (green), or with Δ*dlaT* P. UF1 (blue), and orally infected with Δ*actA L. m*. One group of mice was orally infected with Δ*actA L. m*^{3pep} (grey). Representative data of flow plots, percentage (%), and total cell counts of IL-1β^{+}, IL-6^{+} and IL-12/23p40^{+} DCs. Data are representative of 1 independent experiment (n=4-5 mice/group). Error bars indicate the mean ± S.E.M. **P* < 0.05, ***P* < 0.01, by ANOVA plus Tukey post-test.

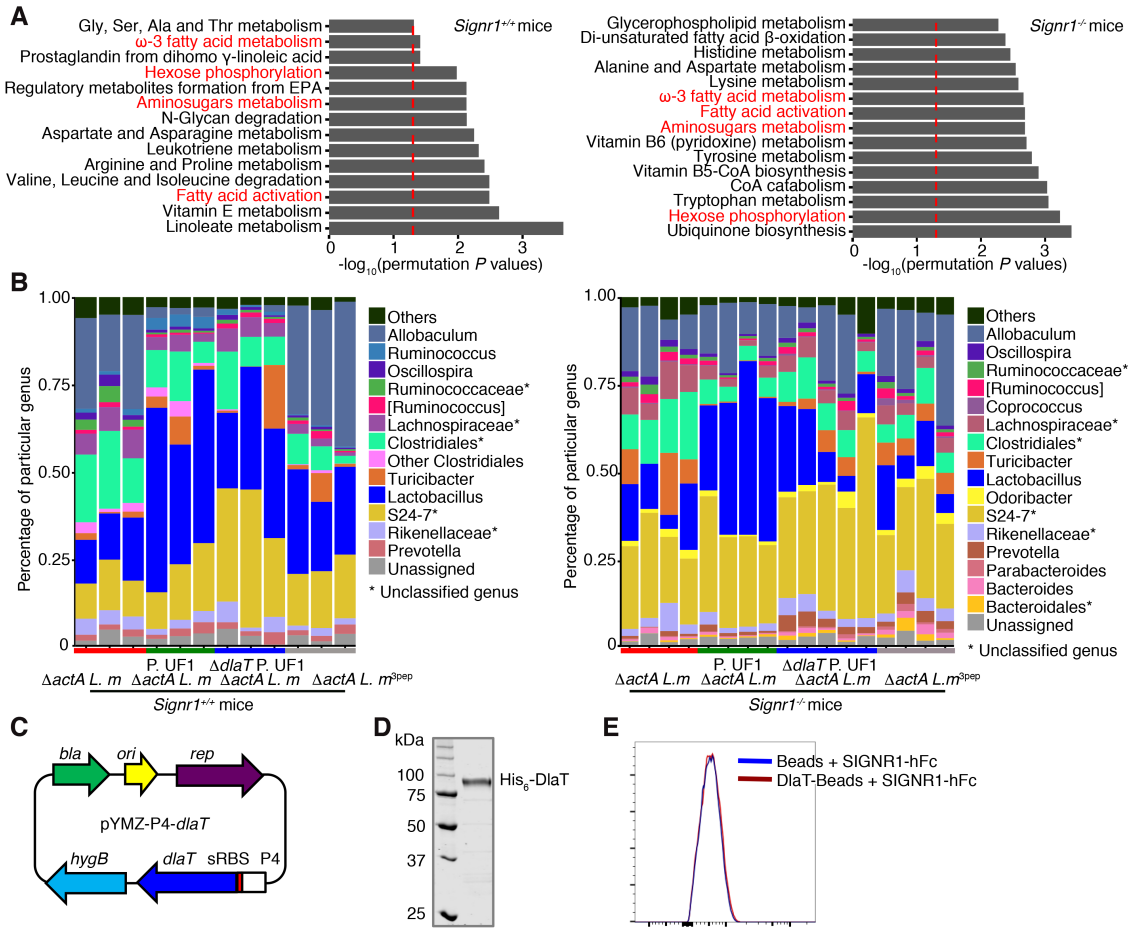

Supplemental Figure 9. Involvement of SIGNR1 in immune regulation during Δ*actA L. m* infection.

(**A** and **B**) *Signr1*$^{-/-}$ or *Signr1*$^{+/+}$ mice were gavaged four times with PBS (red), P. UF1 (green), or Δ*dlaT* P. UF1 (blue), and orally infected with Δ*actA L. m.* One group of mice was infected with Δ*actA L. m*^{3pep} (grey). Pathway analyses of fecal metabolites (**A**) and gut microbiota (**B**) among the aforementioned groups. Red dashed lines indicate permutation $P = 0.05$. (**C**) Plasmid diagram for expressing His_6-DlaT protein in P. UF1 using the P4 promoter and synthetic ribosome-binding site (sRBS). (**D**) SDS-PAGE (10%) analysis of purified His_6-DlaT protein. (**F**) Flow cytometry analysis showing no binding of His_6-DlaT protein to SIGNR1-hFC fusion protein. Representative data of 2 (n=3-5 mice/group, **A** and **B**) or 3 (**D** and **E**) independent experiments.

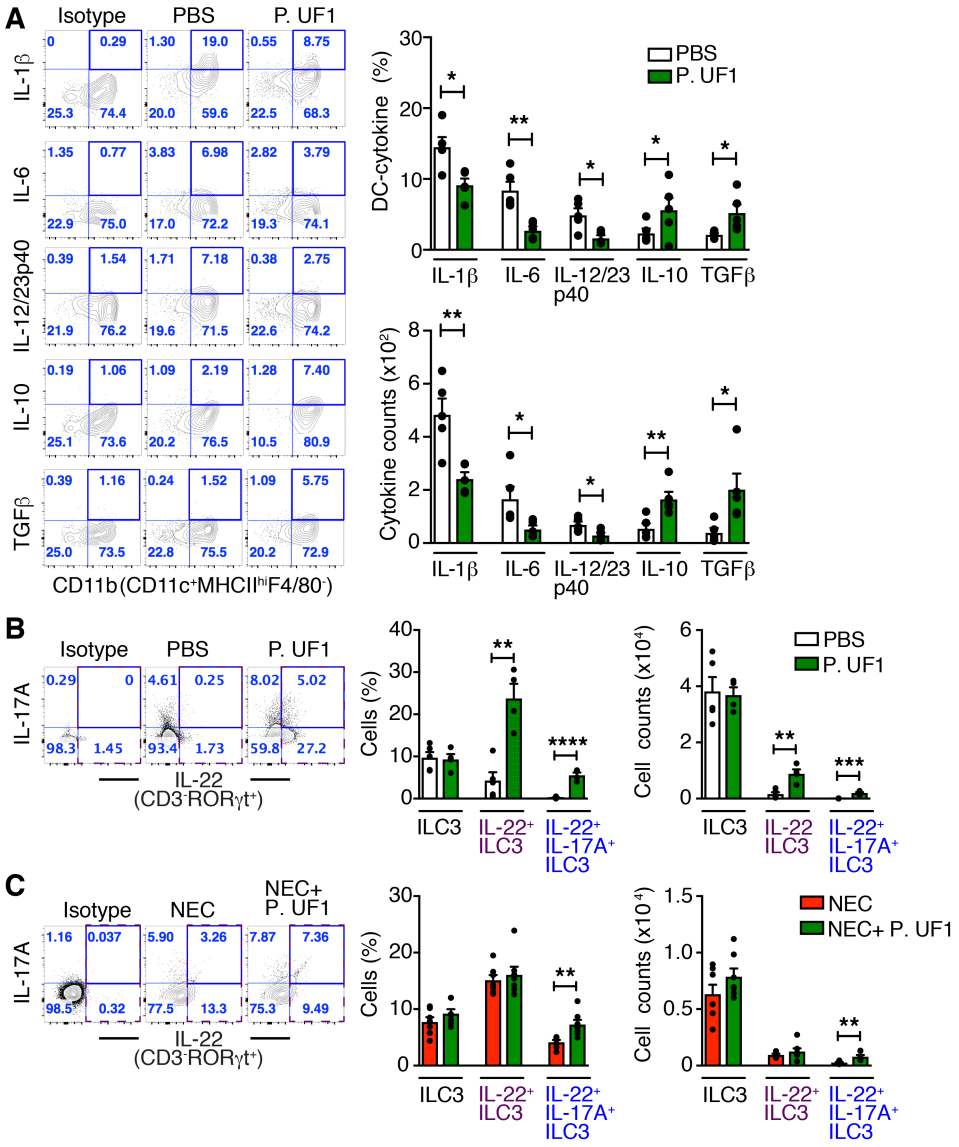

Supplemental Figure 10. Mitigation of NEC-like injury by P. UF1.

(**A**) C57BL/6 pregnant dams were gavaged with P. UF1 or PBS twice a week during the gestation. Five days after birth, newborn mice were sacrificed to evaluate immunity. Representative data of flow plots, percentage (%), and total cell counts of IL-1β^{+}, IL-6^{+} and IL-12/23p40^{+} DCs. Each dot represents three pooled small intestinal tissue samples from each group of the newborn mice. (**B**) Newborn mice of C57BL/6 dams gavaged with P. UF1, or PBS during the pregnancy were gavaged with PBS, or P. UF1 (10^{7} CFU/mouse) on days 6, 8 and 10. Newborn mice were sacrificed on day 12. Representative data of flow plots, percentage (%), and total cell counts of CD3^{-} RORγt^{+} (ILC3), IL-22^{+} ILC3 and IL-17A^{+} IL-22^{+} ILC3. (**C**) Five days after birth, newborn mice of C57BL/6 dams gavaged with P. UF1, or PBS were separated and subjected to experimental NEC-like injury. Newborn mice gavaged with PBS, or P. UF1 (10^{7} CFU/mouse) on days 1, 3 and 5. Newborn mice were sacrificed six days later. Representative data of flow plots, percentage (%), and total cell counts of CD3^{-} RORγt^{+} (ILC3), IL-22^{+} ILC3 and IL-17A^{+} IL-22^{+} ILC3 in newborn mice subjected to NEC-like injury with or without P. UF1 treatment. Data are pooled from 3 experiments in steady state (n=15 newborn mice/group, **A**) or

representative of 2 (n=4-5 mice/group, **B**) or 3 (n=7 mice/group, **C**) independent experiments. Error bars indicate the mean ± S.E.M. *$P < 0.05$, **$P < 0.01$, ***$P < 0.001$, ****$P < 0.001$, by two-tailed unpaired *t*-test (**A-C**).

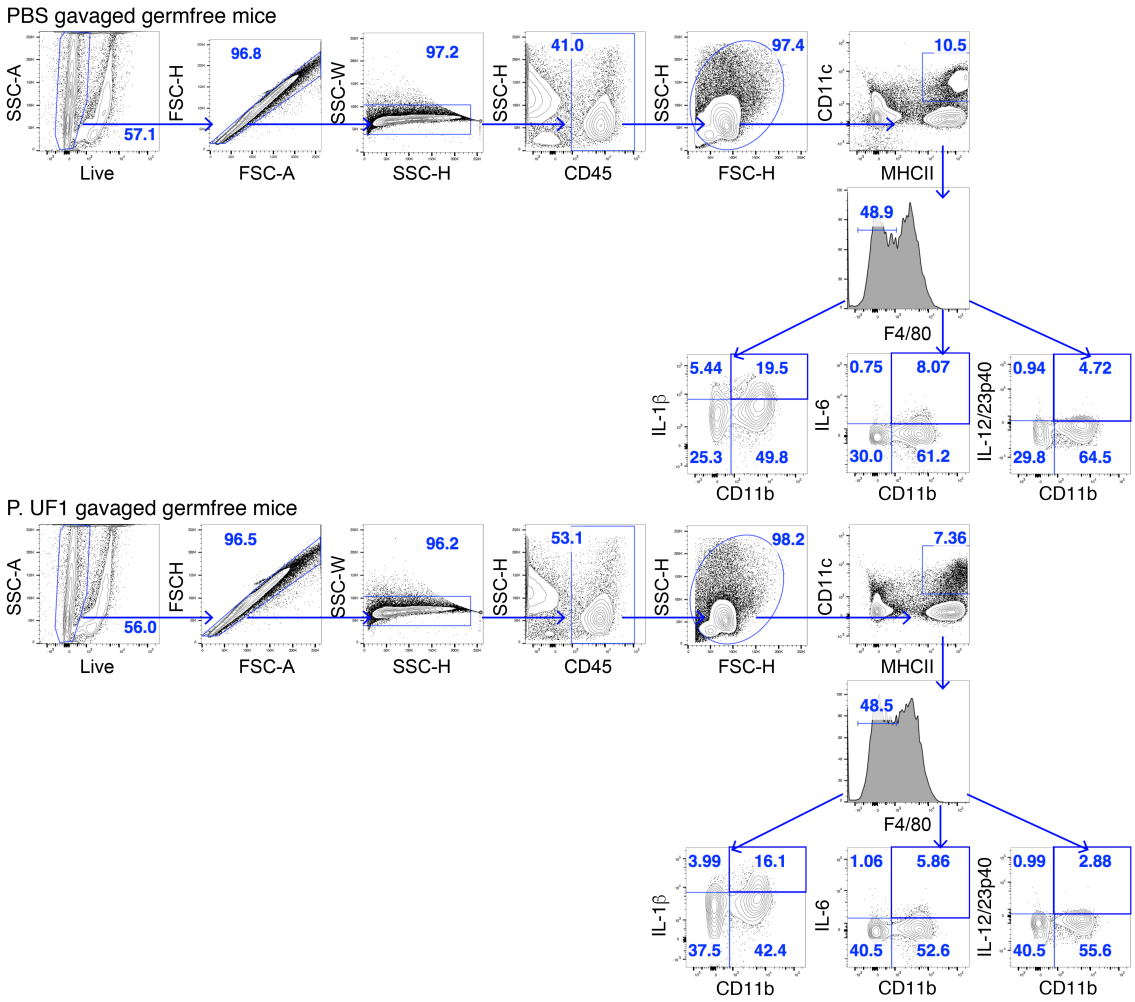

Supplemental Figure 11. Gating strategy for DCs.
GF mice (n=4 mice/group) were gavaged four times with P. UF1, or PBS (10^9 CFU/mouse). Colonic cells were isolated and restimulated with PMA/ionomycin. Cells were stained for flow cytometry analysis. After dead and doublet cell exclusion, $CD45^+$ cells were selected based on their FCS/SSC. DCs were defined as $CD11c^+$ MHC II^{hi} $F4/80^-$ and $CD11b^+$. IL-1β, IL-6 and IL-12/23p40 expression by DCs were then evaluated. Data are depicted in the Supplemental Figure 1B.

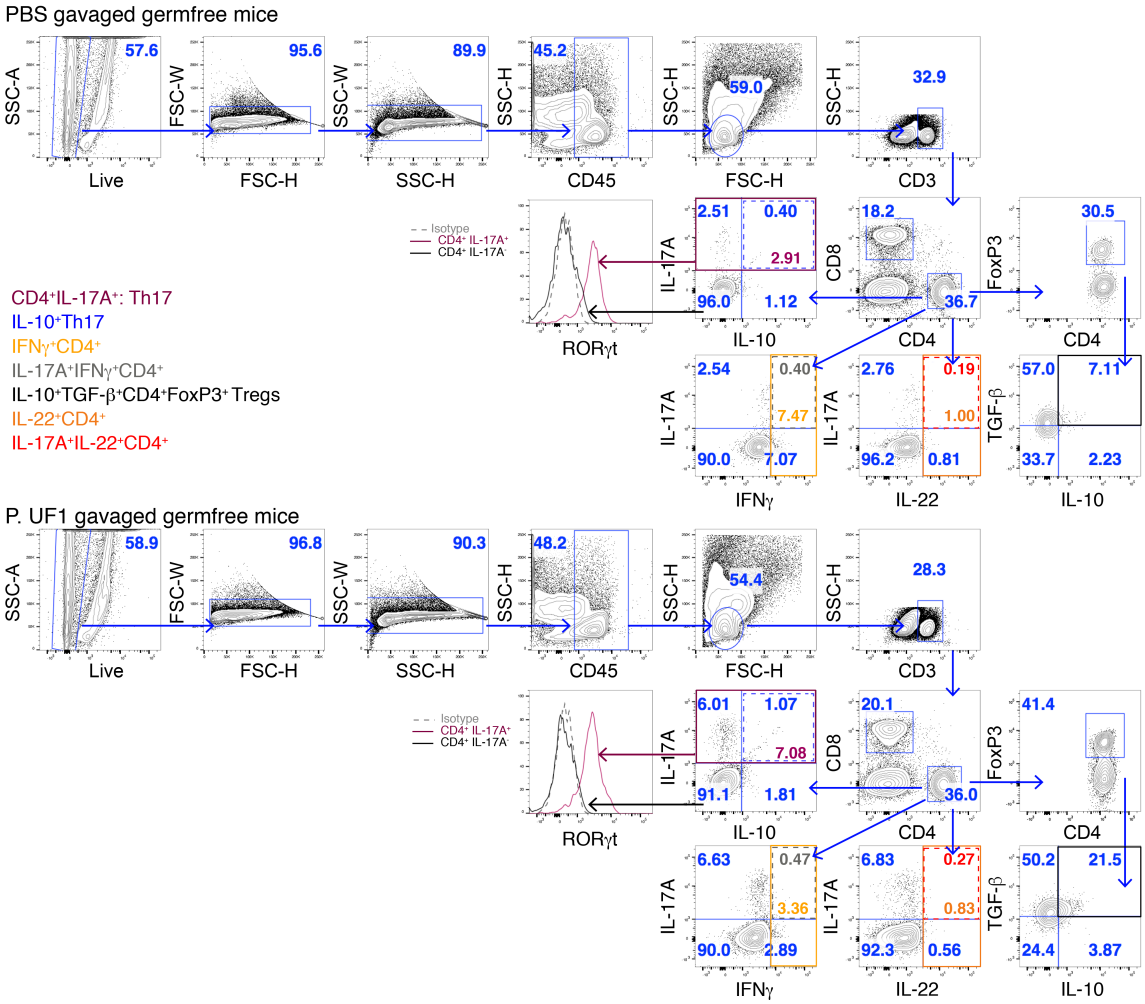

Supplemental Figure 12. Gating strategy for CD4$^+$ T cells.
GF mice (n=4 mice/group) were gavaged four times with P. UF1 or PBS. Colonic cells were isolated and restimulated with PMA/ionomycin. Cells were stained for flow cytometry analysis. After dead and doublet cell exclusion, CD45$^+$ cells were selected based on their FCS/SSC. The levels of IL-10$^+$ IL-17A$^+$ IFNγ$^+$ IL-22$^+$ CD3$^+$ CD4$^+$ CD8$^-$ T cells were evaluated. Tregs were defined as IL-10$^+$ TGF-β$^+$ CD3$^+$ CD4$^+$ CD8$^-$ FoxP3$^+$ cells. Data are depicted in the Figure 3D.

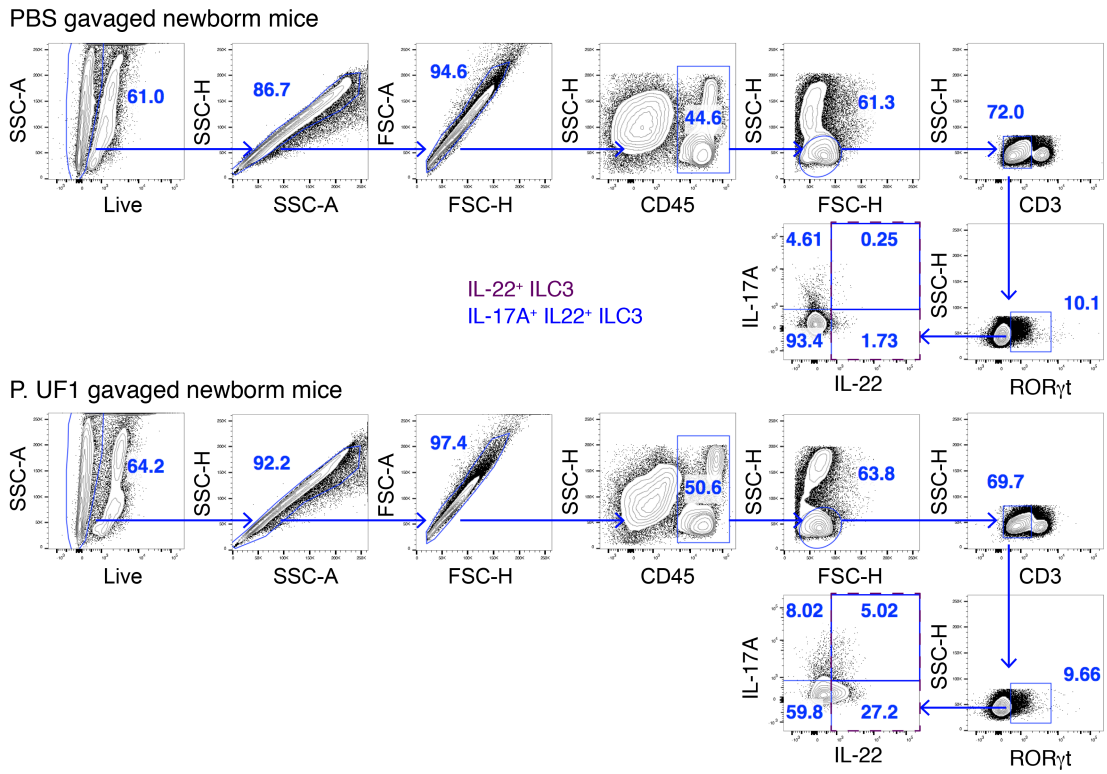

Supplemental Figure 13. Gating strategy for ILC3.

Newborn mice of C57BL/6 dams gavaged with P. UF1, or PBS during the pregnancy were gavaged with PBS, or P. UF1 (10^7 CFU/mouse) on days 6, 8 and 10. Newborn mice were sacrificed on day 12. Small intestinal cells were isolated and restimulated with PMA/ionomycin. Cells were stained for flow cytometry analysis. After dead and doublet cell exclusion, $CD45^+$ cells were selected based on their FCS/SSC. ILC3 were defined and plotted as $CD3^-$ $ROR\gamma t^+$ $IL\text{-}17A^+$ $IL\text{-}22^+$ ILC3. Data depicted in the Supplemental Figure 10B.